International Journal of Electrical Engineering.
ISSN 0974-2158 Volume 4, Number 4 (2011), pp. 499-510
© International Research Publication House
http://www.irphouse.com

High Frequency Modeling of Two Limb Series Loop Winding for Partial Discharge Localization

Santosh Kumar Annadurai[1] and Udayakumar K.[2]

[1]CG Global R&D Centre,
Crompton Greaves Ltd, Kanjur Marg, Mumbai, India
[2]Division of High Voltage Engineering,
Anna University, Chennai, India
E-mail: santosh.annadurai@cgglobal.com

Abstract

Partial discharge (PD) measurement is widely accepted as a quality control test to study and detect the incipient insulation faults in power system equipments. This paper describes the study of partial discharge propagation behavior in a 6kV / 60kVA two limb series limb type winding by comparing between the PD location estimated by simulated equivalent circuit and experimental estimation by terminal current measurement method. The winding considered has 6 accessible taps hence the simulation is also done in 12 parts to simulate injection of PD pulses at various location to cross check with actual results. The design parameters are used to derive the high frequency equivalent circuit by simulating in software packages such as ANSOFT & MAGNET and also analytical calculation methods. The high frequency equivalent circuit of the winding consists of series inductance (L), capacitance (Cs), and ground capacitance (Cg) of the winding [1]. The equivalent circuit is simulated in PSPICE and standard PD signal is injected at various locations (6 locations). The response signals at start and end terminals of circuit are captured and analyzed in the frequency domain & the location is estimated by the formula using the series resonance frequency methodology [2]. Experiments are conducted by injecting PD pulses into the winding at various tap locations using pulse generator, the traveled signals at the line and neutral end terminals are captured using High frequency current transformer (HFCT). The frequency spectra of the measured signals at line and neutral end for various tap locations along the winding height are analyzed and similarly the PD location is estimated, compared and validated with the location

estimated by the simulated transformer winding equivalent circuit model in PSPICE. The effect of PD location in transformer winding on the propagation of partial discharge pulses and its effect on the frequency response and the accuracy of the PD location estimation are illustrated.

Keywords: Partial discharges, high frequency modeling, Partial discharge propagation, HFCT, Partial discharge localization.

Introduction

Partial discharges (PD) are localized electrical breakdown within the insulation, which do not bridge the end electrodes. During the occurrence of PD energy dissipation takes place and can be attributed to various kinds of generated signals such as electrical current pulses through earth, voltage drop across electrodes, electromagnetic radiations, optical signal and acoustic energy emission simultaneously. Furthermore, PD is also attributed to post effect which is reflected in chemical property of insulation oil (Dissolved Gas Analysis). PD measurements can be conducted either continuously or intermittently and on-line or off-line. PD results are a reliable source to assess the health of electrical equipment and to plan for maintenance.

Electrical PD detection methods are classified as conventional offline method [2] which, measures apparent charge quantity using conventional PD measuring circuitry and instruments with a centre frequency of 500 kHz and 250 kHz for narrowband method and wideband methods respectively [10]. PD type and location can be determined by analyzing the shape of the captured PD signal in time domain. The other electrical method captures the earth current and bushing current signals propagated along the winding height is preferable for online monitoring. Recent developments in electrical methods are based on the fact that while a discharge signal propagates from the location to the measuring terminals, the terminal response acquires the information on the location of the PD source. The PD type and location can be determined by frequency spectrum analysis of the captured signal.

Lumped parameter model for transformer winding

Consider the high frequency equivalent model of a transformer winding shown in fig.1, the high frequencies in the measurement is due the capacitance present between transformer windings and earthed parts (core, tank, etc.), within each winding between discs, turns and layers, and between individual coils. Owing to this capacitance the voltage distribution of steep-front over voltages within the transformer will not be uniform [7]. A section of the model two of its element, each of its length *dx*, the inductance of each element is denoted by L (H m^{-1}), its shunt capacitance by Cg (F m^{-1}), and its series capacitance by Cs (F m).

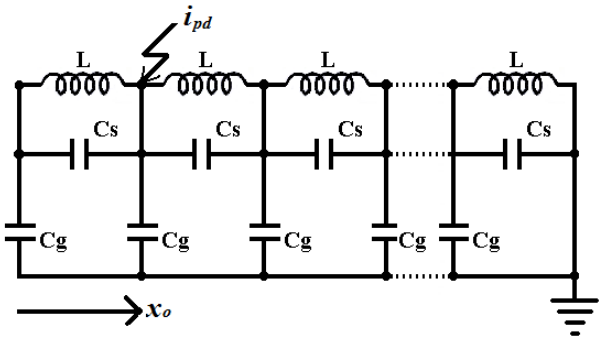

Figure 1: Lumped parameter model of a single layer transformer winding.

In this work a 6kV / 60kVA transformer consisting of two limb series loop type winding with six accessible taps was designed for the experimentation. Each tapings are uniformly arranged by disc position spacing. The inductance value of each crossover coil calculated using Grover method and shown in table.1.

Table 1: The equivalent inductances of each crossover coil.

$L_{A1} = 6.433926094$	$L_{B1} = 6.616437978$	$L_{C1} = 6.894994612$
$L_{D1} = 6.894994612$	$L_{E1} = 6.989123142$	$L_{F1} = 7.083889832$
$L_{A2} = 6.894994612$	$L_{B2} = 6.894994612$	$L_{C2} = 6.894994612$
$L_{D2} = 6.894994612$	$L_{E2} = 7.083889832$	$L_{F2} = 6.894994612$

The series and shunt capacitances have been derived from the simulation in MAXWELL, ANSOFT software. The series capacitances (in Farads) are as given below:

Capacitance between discs $A_2 - A_1$: 1.5353 e-11
Capacitance between discs $A_1 - B_2$: 1.6980 e-11
Capacitance between discs $B_2 - B_1$: 1.9217 e-11
Capacitance between discs $B_1 - C_2$: 2.2590 e-11
Capacitance between discs $C_2 - C_1$: 2.8371 e-11
Capacitance between discs $C_1 - D_2$: 3.3129 e-11
Capacitance between discs $D_2 - D_1$: 2.8403 e-11
Capacitance between discs $D_1 - E_2$: 2.2646 e-11
Capacitance between discs $E_2 - E_1$: 1.9276 e-11
Capacitance between discs $E_1 - F_2$: 1.6916 e-11
Capacitance between discs $F_2 - F_1$: 1.5307 e-11

The shunt capacitances (in Farads) are as given below:

Ground capacitance for disc A_2 : 1.0468 e-10
Ground capacitance for disc A_1 : 1.0502 e-10

Ground capacitance for disc B_2 : 7.8525 e-11
Ground capacitance for disc B_1 : 7.8209 e-11
Ground capacitance for disc C_2 : 7.3606 e-11
Ground capacitance for disc C_1 : 7.2830 e-11
Ground capacitance for disc D_2 : 7.3588 e-11
Ground capacitance for disc D_1 : 7.2865 e-11
Ground capacitance for disc E_2 : 7.8855 e-11
Ground capacitance for disc E_1 : 1.053 e-11

Series resonance method for Location of PD

If PD may occur in section x_0, the differential equations describing the transient process taking place in the winding, and based on the Kirchhoff's laws, takes the following form:

$$\frac{\partial i_L}{\partial x} + \frac{\partial i_{Cs}}{\partial x} = -C_g \frac{\partial u}{\partial t} \tag{1}$$

$$i_{Cs} = Cs \frac{\partial^2 u}{\partial x \partial t} \tag{2}$$

$$\frac{\partial u}{\partial x} = -L \frac{\partial i_L}{\partial t} \tag{3}$$

The current and voltages appearing in the above relation are functions of the space and time, by eliminating the currents; the above equations can be reduced to a single differential equation of 4th order referring to the voltage:

$$\frac{\partial^2 u}{\partial x^2} - LC_g \frac{\partial^2 u}{\partial t^2} + LC_s + \frac{\partial^4 u}{\partial x^2 \partial t^2} = 0 \tag{4}$$

The voltage and current distribution along the winding are given by equations (5) and (6) [8]:

$$u(x, j\omega) = A\cosh(\gamma x) + B\sinh(\gamma x) \tag{5}$$

$$i(x, j\omega) = \frac{1}{Z}\left[A\sinh(\gamma x) + B\cosh(\gamma x)\right] \tag{6}$$

According to the standing wave theory [8] the waves are produced of frequency $\frac{\omega}{2\pi}$ in time and of $\frac{\gamma}{2\pi}$ frequency in space. Between angular frequencies ω in time γ in space the following relations prevail:

$$\omega = \frac{\gamma}{\sqrt{LC\left(1 + \frac{C_s}{C_g}\gamma^2\right)}} \tag{7}$$

$$\gamma = \sqrt{\frac{LC_g\omega^2}{1-\omega^2 LC_s}} \text{ and} \tag{8}$$

$$Z = \sqrt{\frac{L}{C\left(1-LC_s\omega^2\right)}} \tag{9}$$

The equations (5) and (6) clearly shows the voltage and current of the windings are relate with the angular frequencies and length of the winding. So by taking the length of the wining as unit length, when a PD current i_{pd} occurs at x_0, from the line end, the voltage and current distribution along the winding due to the PD source will be described as similar to equations (5) and (6).

Therefore the voltage and current distribution can be written as,

At line end to PD occurrence:

$$u_1(x, j\omega) = A_1 \cosh(\gamma(x_0 - x)) + B_1 \sinh(\gamma(x_0 - x)), \text{ for } 0 \le x \le x_0 \tag{10}$$

$$i_1(x, j\omega) = \frac{1}{Z}\left[A_1 \sinh(\gamma(x_0 - x)) + B_1 \cosh(\gamma(x_0 - x))\right], \text{ for } 0 \le x \le x \tag{11}$$

At PD occurrence to neutral:

$$u_2(x, j\omega) = A_2 \cosh(\gamma(x - x_0)) + B_2 \sinh(\gamma(x - x_0)), \text{ for } x_0 \le x \le 1. \tag{12}$$

$$i_2(x, j\omega) = \frac{1}{Z}\left[A_2 \sinh(\gamma(x - x_0)) + B_2 \cosh(\gamma(x - x_0))\right], \text{ for } x_0 \le x \le 1. \tag{13}$$

Where the constants A1, B1, A2, and B2 can be determined by the boundary conditions of the winding given by

$$i_1(0, j\omega) = j\omega . C_b . u_1(0, j\omega) \tag{14}$$

$$i_{pd} = i_1(x_0, j\omega) + i_2(x_0, j\omega) \tag{15}$$

$$u_2(1, j\omega) = 0 \tag{16}$$

By solving (10) to (13) with the boundary conditions in equations (14) to (16) an analytical solution for the line end current can be obtained in equation (17) is given by,

$$i_1(j\omega) = \frac{\frac{C_b}{C_g}\gamma \sinh(\gamma(1 - x_0))}{-\cosh(\gamma) + \frac{C_b}{C_g}\gamma \sinh(\gamma)} i_{pd} \tag{17}$$

Where, C_b is the simulated bushing capacitance in the line end terminal. The equation (17) clearly shows as the transfer function of the line end discharge signal contain the information of the discharge itself i_{pd} and its location x_0. So from this

analysis we have to conclude that the location of the PD x_0 is relates with the series resonance frequencies of the measured signal.

PD calibration assumes the discharge source at the line-end, i.e. x_0, and therefore equation (24) simplifies to

$$LC + n^2\pi^2 LK = \left(\frac{n}{2f}\right)^2 \tag{18}$$

Equation (20) shows that if two series resonances f_1 and f_2 can be obtained corresponding to n_1 and n_2, then LC_g and LC_s can be found for the equivalent circuit of the winding and are given by

$$LC_g = \frac{(n_1 n_2)^2}{4(n_2^2 - n_1^2)}\left(\frac{1}{f_1^2} - \frac{1}{f_2^2}\right) \tag{19}$$

$$LC_s = \frac{1}{4\pi^2(n_2^2 - n_1^2)}\left[\left(\frac{n_2}{f_2}\right)^2 - \left(\frac{n_1}{f_1}\right)^2\right] \tag{20}$$

The position of unknown PD is obtained from LC_s, LC_g equation is given by,

$$x_0 = 1 - \frac{n}{2f}\sqrt{\frac{1 - 4\pi^2 f^2 LC_s}{LC_g}} \tag{21}$$

Simulation of PD pulse propagation in 60 kVAr Reactor winding

The parameters of the high frequency which are derived from the analytical methods are used to simulate the winding in PSPICE to study the partial discharge waveform propagation in the winding. The simulated PD pulse is as shown in the fig.2 and the waveforms as captured at winding bushing end and its corresponding Fast fourier transform (FFT) as shown in fig 3 & 4 respectively. Table 2 shows the resonant frequencies of the winding due to injection of simulated PD pulse across the tapping of the winding.

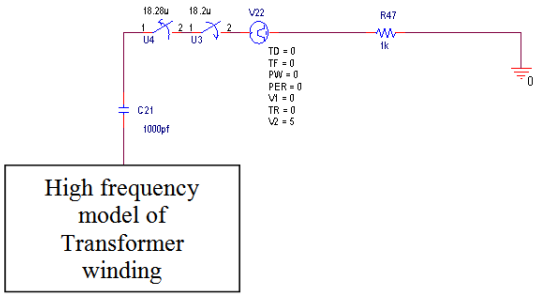

Figure 2: PSPICE Simulation model with simulated PD source injected between each section.

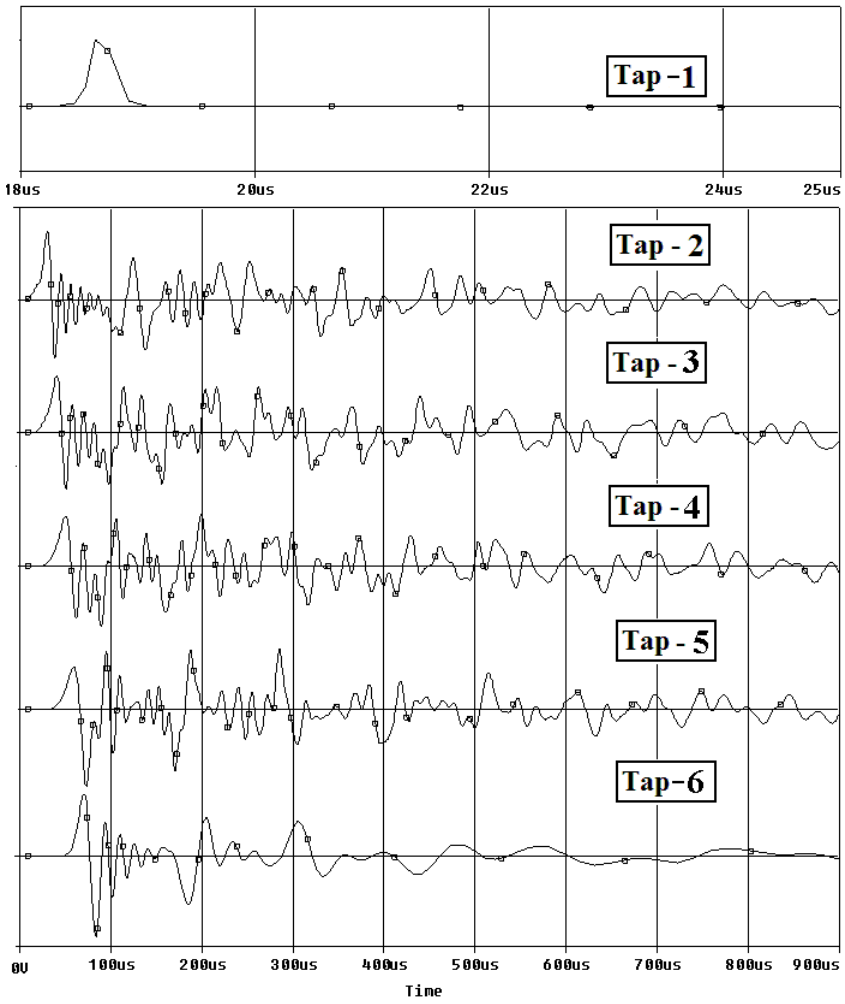

Figure 3: Measured wave while PD injected each section of the simulation model.

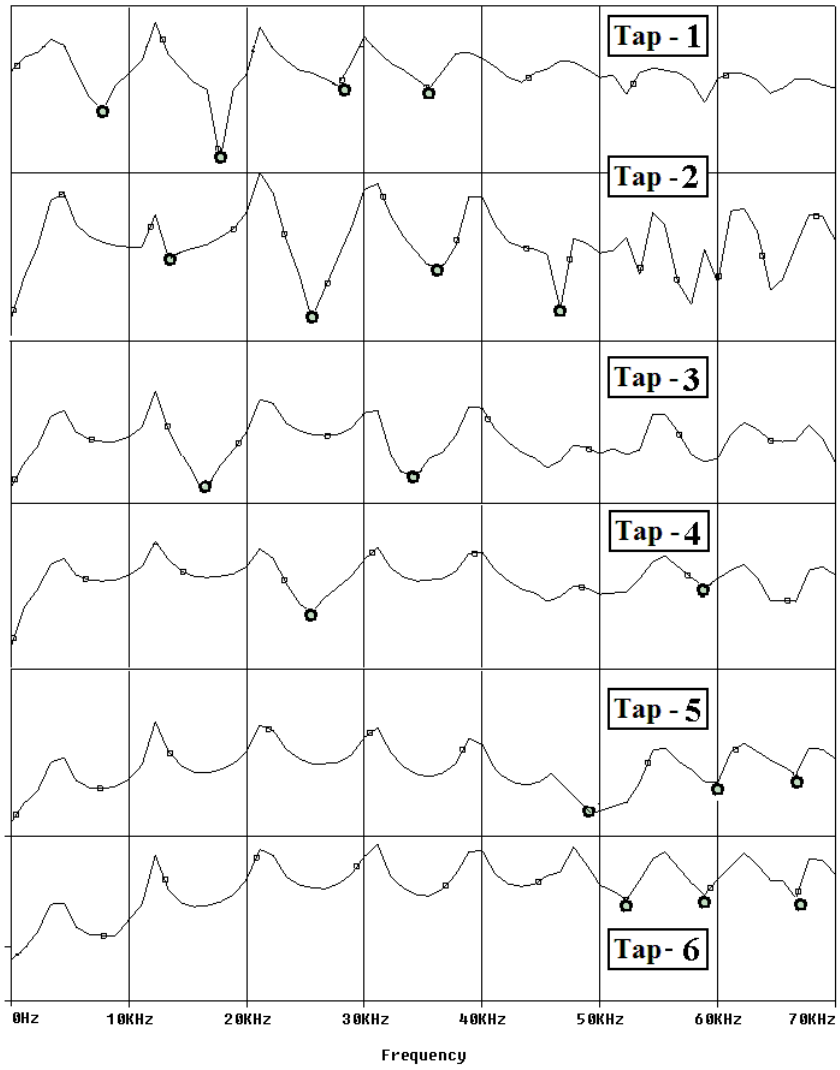

Figure 3: Frequency spectra of the measured signal.

Table 2: Series resonant frequency for the signals measured at Bushing tap for various tap positions.

	Series resonance frequencies			
	F1	F2	F3	F4
Tap 0	8.5	18	29	36
Tap 1	10.5	26	37	46
Tap 2	13.5	34		
Tap 3	20	59.5		
Tap 4	42	66		
Tap 5	53			

From the above tabulation the calculated equivalent product of inductance with Series and Shunt capacitances are as follows:

LC_s = 3.5848E-09

LC_g = -1.26242E-11

Table 3: Comparison table of location estimated Vs actual.

Tap No	Actual PD positon (%)	Estimated position due to F1 (%)	Error (%)
Tap 0	0	0	0
Tap 1	16.667	18.311	9.864
Tap 2	33.33	35.393	6.19
Tap 3	50	54.272	8.544
Tap 4	66.66	72.744	9.127
Tap 5	83.333	75.59	-9.292

The location algorithm gave a PD location estimate within ± 10% of the winding height.

Experimentation

A simplified block diagram of the measurement system is shown in fig.4. The experimental setup consists of a PC based NI-Real time Data acquisition system (DAQ) with sampling rate of 100 Ms/s, 1:10 probes and PD calibrator. Using the PD calibrator typical PD pulses of 1000pC was injected into each tapings of the winding and corresponding response signals from all the tapings are recorded. 50Ω resistors are used to prevent reflection of the signal attenuation when connected to cables with characteristic impedance. They also act as detection impedance for PD signals. These resistors have constant characteristics over a wide frequency range in order to avoid affecting the frequency response of the coil.

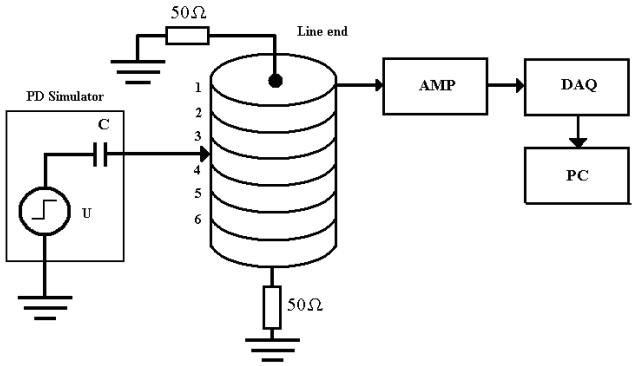

Figure 4: Experimental set-up used for discharge detection on 6 kV transformer winding.

AMP – Inbuilt probe amplifier.

DAQ – NI Real time Data Acquisition System

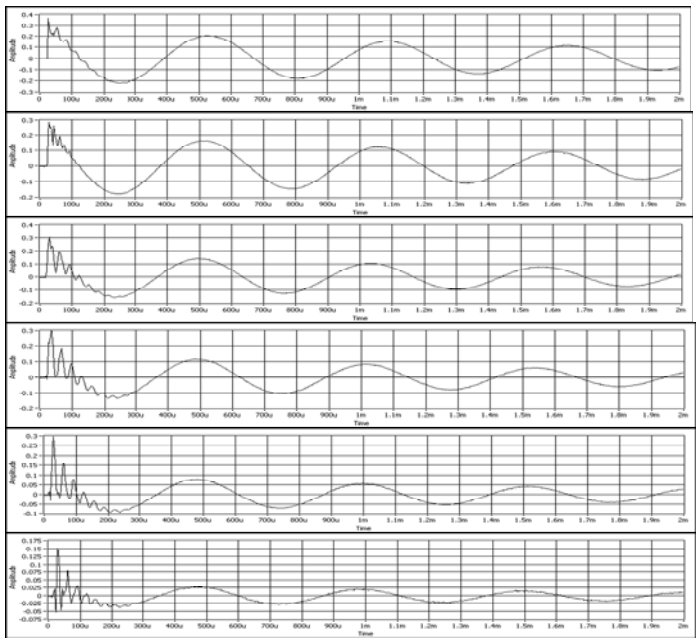

Figure 5: Measured signals when PD calibrator is connected to all the tapings (sampling rate 100MS/s)

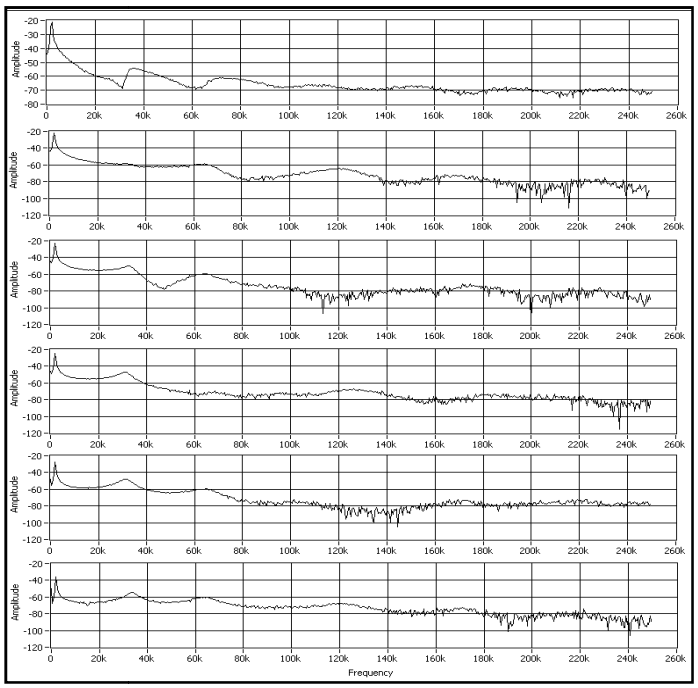

Figure 12: Frequency spectra of measured signals at line end (in dB).

Table 4: Position of measured poles (khz).

Poles order.	1	2	3	4	5	6
Frequency (kHz)	2	32	65	72	110	180

Table 5: Position of troughs in captured line-end signals.

PD position	Series Resonance Frequencies (kHz)				
	f 1	f2	F3	f4	f5
Tap 0	32	62	100	140	170
Tap 1	38	80	140	-	-
Tap 2	48	112	-	-	-
Tap 3	60	80	-	-	-
Tap 4	90	144	-	-	-
Tap 5	150	-	-	-	-

Estimation of PD Location from Series Resonant Frequency

$$LC_g = \frac{(n_1 n_2)^2}{4(n_2^2 - n_1^2)}\left(\frac{1}{32^2} - \frac{1}{62^2}\right)$$

Using equations 19, 20 & 21 the estimated PD locations for the simulated winding w.r.t the actual PD location is as given in the table.6.

Table 6: Location of PD pulses in various tapings.

Tap Number	Actual PD position in % height	Measured position in % height (simulation)	Error (%)	Measured position in % height (experiment)	Error (%)
Tap 0	0	0	-	0	-
Tap 1	16.667	18.311	*9.864*	16.176	-2.946
Tap 2	33.333	35.393	6.19	34.271	2.814
Tap 3	50	54.272	8.544	48.187	*-3.626*
Tap 4	66.667	72.744	9.124	67.304	0.955
Tap 5	83.333	75.59	-9.292	84.448	1.338

The location algorithm gave a PD location estimate within ± 4% of the winding height as per the experimental results vis-à-vis ± 10% for the simulated equivalent winding.

Conclusion

Partial discharge propagation behavior in a 6kV / 60kVA two limb series limb type winding with six accessible taps has been done for both experimentally and also using the design parameters of the winding the high frequency equivalent circuit is derived by analytical methods. The partial discharge location estimated by both methods showed an accuracy of less than ±10%. Accuracy derived from experimentation is less than ±4% and of analytical method is ±10%. This variation in the accuracy is attributed to the complexity in modeling a complex geometry such as two limb series loop winding, the assumptions and the rounding off done during derivation of the equivalent circuit. In this work the high frequency equivalent circuit and partial discharge location algorithm have been evaluated for a complex two limb series loop winding. This work is further extended into development of an partial discharge monitoring system having intelligent location software developed based on this evaluated algorithm.

References

[1] Asghar Akbari, Peter Werle, Hossein Borsi, and Ernst Gockenbach, 'Transfer function-based partial discharge localization in power transformers: A feasibility study', IEEE Electrical Insulation Magazine sep/oct 2002.

[2] British Standard BS EN 60270:2001, "High – Voltage Test Techniques-Partial Discharge Measurements", (IEC60270:2000), 2001.

[3] M.D. Judd, B.M. Pryor, S.C. Kelly and B.F. Hampton, "Transformer Monitoring Using the UHF Technique", Intern. Symposium. High Voltage (ISH1999), London, UK, Vol. 5, pp.362-365, 1999.

[4] S.N. Hettiwatte, P.A. Crossley, Z.D. Wang, A. Darwin and G.Edwards, 'Simulation of a transformer winding for partial discharge propagation studies', IEEE Power Engineering Society Winter meeting 2002, New York, USA.

[5] S.N. Hettiwatte, P.A. Crossley, Z.D. Wang, A. Darwin and G.Edwards, 'Experimental investigation into the propagation of partial discharge pulses in transformers', IEEE Power Engineering Society Winter Meeting, 2002.

[6] Z.D. Wang, P.A. Crossley, K.J. Cornick and D.H. Zhu, ' Partial discharge location in power transformers', IEE Proceedings on Science, Measurement and technology September 2000.

[7] K. Karsai, D. Kerenyi and L. Kiss, Large Power Transformers, ELSEVIER, Amsterdam 1987.

[8] H.S. Carslaw and J.C. Jaeger, Operational Methods in Applied Mathematics, Dover Books, 1977.

[9] Heller, B. and Veverka, A. (1968): Surge Phenomena in Electric Machines. Academia, Prague.

[10] M.S. Naidu and V. Kamaraju, High Voltage Engineering, Tata McGraw-Hill Publishing Company Limited, 2004.